FGF-1 induces ATP release from spinal astrocytes in culture and opens pannexin and connexin hemichannels

Juan M. Garré[a,b], Mauricio A. Retamal[c,d], Patricia Cassina[a], Luis Barbeito[e,f], Feliksas F. Bukauskas[b], Juan C. Sáez[b,c,d], Michael V. L. Bennett[b,1,2], and Verónica Abudara[a,1,2]

[a]Facultad de Medicina, Universidad de la República Oriental del Uruguay, C.P. 11800 Montevideo, Uruguay; [b]The Albert Einstein College of Medicine, Bronx, NY 10461; [c]Departamento de Fisiología, Pontificia Universidad Católica de Chile, Santiago 6513677, Chile; [d]Núcleo Milenio de Inmunología e Inmunoterapia, Santiago 6513677, Chile; [e]Instituto de Investigaciones Biológicas Clemente Estable, C.P. 11600 Montevideo, Uruguay; and [f]Institut Pasteur Montevideo, C.P. 11400 Montevideo, Uruguay

Contributed by Michael V. L. Bennett, September 16, 2010 (sent for review March 1, 2010)

Spinal astrocytes are coupled by connexin (Cx) gap junctions and express pannexin 1 (Px1) and purinergic receptors. Fibroblast growth factor 1 (FGF-1), which is released in spinal cord injury, activated spinal astrocytes in culture, induced secretion of ATP, and permeabilized them to relatively large fluorescent tracers [ethidium (Etd) and lucifer yellow (LY)] through "hemichannels" (HCs). HCs can be formed by connexins or pannexins; they can open to extracellular space or can form gap junction (GJ) channels, one HC from each cell. (Pannexins may not form gap junctions in mammalian tissues, but they do in invertebrates). HC types were differentiated pharmacologically and by Px1 knockdown with siRNA and by use of astrocytes from Cx43 knockout mice. Permeabilization was reduced by apyrase (APY), an ATPase, and by $P2X_7$ receptor antagonists, implicating secretion of ATP and autocrine and/or paracrine action. Increased permeability of cells exposed to FGF-1 or ATP for 2 h was mediated largely by Px1 HCs activated by $P2X_7$ receptors. After a 7-h treatment, the permeability was mediated by both Cx43 and Px1 HCs. FGF-1 also caused reduction in gap junctional communication. Botulinum neurotoxin A, a blocker of vesicular release, reduced permeabilization when given 30 min before FGF-1 application, but not when given 1 h after FGF-1. We infer that ATP is initially released from vesicles and then it mediates continued release by action on $P2X_7$ receptors and opening of HCs. These changes in HCs and gap junction channels may promote inflammation and deprive neurons of astrocyte-mediated protection in spinal cord trauma and neurodegenerative disease.

astroglia | growth factor | connexon | pannexon | neurodegeneration

Connexins (Cxs) form gap junctions (GJs) in vertebrates whose function at many sites is direct intercellular communication between the contacting cells (1). GJs between neurons comprise one form of electrical synapse; GJs between astrocytes allow passage of ions and small molecules that coordinate numerous cell functions (2). Cx hemichannels (HCs) in nonjunctional membrane can be "functional" in that they can open connecting cell interior and extracellular milieu (3). In cultured cortical astrocytes, Cx43 HCs provide a pathway for uptake and release of small molecules, including tracers to which GJs are permeable and small organic molecules such as ATP, NAD^+, glutamate, glucose, and prostaglandins (4). Opening of HCs appears involved in many physiological and pathological cell responses, including volume regulation, proliferation, calcium wave propagation by extracellular messengers, and cell death during metabolic inhibition (3).

Recently, expression of pannexin 1 (Px1) was found in cortical astrocytes (5). Px1 is a member of the pannexin family of proteins, which form GJs in invertebrates, where the proteins are also called innexins. Px1 forms hemichannels (HCs), or pannexons, that open in nonjunctional surface membrane in several vertebrate cell types, including *Xenopus* oocytes (6), mammalian neurons (7), and HEK293 cells (8). Expression of Px1 can induce electrical coupling of *Xenopus* oocytes (6) and C6 glioma cells (9), presumably via GJs, although ultrastructural data are lacking. However, Px1 may not form GJs in mammalian tissues (7).

In addition to Cxs and Px1, spinal astrocytes express $P2X_7$Rs and P2YRs (10). During sustained application of ATP, $P2X_7$Rs may trigger permeation of relatively large molecules including ethidium$^+$ (Etd^+) (11) and allow the release of ATP (12). This response was thought to result from channel dilation; however, single channel conductance and reversal potential do not change during ATP treatment (13), and a more likely mechanism is the opening of Px1 HCs induced by P2YRs or $P2X_7$Rs when they bind ATP (8, 12) (however, see ref. 14). Proinflammatory molecules such as bacterial lipopolysaccharide and basic fibroblast growth factor 2 (FGF-2) enhance ATP release via Cx HCs in Cx43-expressing C6 glioma cells (15). Moreover, in cortical astrocytes the activity of at least Cx43 HCs is enhanced in two proinflammatory conditions, application of TNF-α and IL-1β (16) and oxygen/glucose deprivation (4). After injury or trauma, inflammatory mediators, such as ATP, are released by reactive microglia and astrocytes as well as dying neurons, and accumulated ATP may cause neuronal death via $P2X_7$R activation (17). Conversely, sublethal ischemia (preconditioning) increases the number of surface Cx43 HCs and leads to the release of ATP from astrocytes and accumulation of its catabolite, adenosine, which may protect neurons from subsequent ischemic insults (18).

The acidic fibroblast growth factor, FGF-1, is also inflammatory in the adult spinal cord, and, as for ATP, its extracellular level is increased in response to cell injury (19, 20). FGF-1 activates spinal astrocytes, and activated astrocytes are implicated in neurodegenerative disorders such as amyotrophic lateral sclerosis (21, 22). To explore inflammatory mechanisms in spinal cord, we used rat and mouse spinal astrocytes in culture. FGF-1 induced the release of ATP and the opening of Px1 HCs via $P2X_7$Rs. This opening underlay an early (2 h) increase in membrane permeability by autocrine/paracrine action of the released ATP. By 7 h, both Px1 HCs and Cx43 HCs contributed to the increased membrane permeability. These changes were accompanied by reduction in dye coupling via (connexin) GJs, which also depended on ATP release. Autocrine/paracrine effects of ATP are likely relevant to disease processes in the spinal cord in neurodegeneration and after trauma.

Author contributions: J.M.G., M.A.R., P.C., L.B., F.F.B., J.C.S., M.V.L.B., and V.A. designed research; J.M.G., M.A.R., P.C., F.F.B., and V.A. performed research; J.M.G., M.A.R., L.B., F.F.B., J.C.S., M.V.L.B., and V.A. analyzed data; and J.M.G., F.F.B., J.C.S., M.V.L.B., and V.A. wrote the paper.

The authors declare no conflict of interest.

[1]M.V.L.B. and V.A. contributed equally to this work.

[2]To whom correspondence may be addressed. E-mail: michael.bennett@einstein.yu.edu or abudara@fmed.edu.uy.

This article contains supporting information online at www.pnas.org/lookup/suppl/doi:10.1073/pnas.1013793107/-/DCSupplemental.

Results

FGF-1 Induces Spinal Astrocytes to Take up Etd^+ and Lucifer Yellow^{2-} (LY^{2-}), Two GJ Permeant Tracers. Confluent cultures of spinal astrocytes were exposed to 10 ng/mL FGF-1 and 5 IU/mL heparin for varying periods. We used a single application; activity FGF-1 with heparin lasts over 24 h, although only 30–60 min in its absence (23). Initially, we evaluated membrane permeability by dye uptake using a 5-min simultaneous application of LY^{2-} (0.5 mM) and Etd^+ (5 μM) followed by washing and fluorescence imaging. Cultures showed increased uptake of Etd^+ and LY^{2-} after 2- and 7-h FGF-1 treatments (Fig. S1*A*). The two dyes were partially colocalized in single cells. Uptake depended on FGF-1 concentration, and responses to 10 ng/mL were near maximal (24). Whereas control or 2-h FGF-1–treated cells were flat, most cells after 7 h of FGF-1 treatment were reactive, i.e., their cytoplasm was retracted around the nucleus leaving thin connections between cells (Fig. S1, black arrows in 7-h phase image and Fig. S7*A*) (see ref. 21).

FGF-1–Induced Increase in Membrane Permeability Is at First Mediated by Px HCs; by 7-h Treatment, both Px and Cx HCs Contribute. In our initial studies, cultures were treated with FGF-1 for varying times and LY^{2-} uptake was measured as for Fig. S1. By this method uptake was significant after 0.5–2 h of FGF-1 treatment, maximal after 4–7 h, and decreased to near control after 15 h and 40 h, the longest interval tested (Fig. 1*A*). Because of the high fluorescence of LY^{2-} in solution, we did not attempt to quantify dye uptake in the presence of LY^{2-} in the medium, an approach that is convenient for Etd^+, which shows very little fluorescence until bound to intracellular material (25). To acquire quantitative data on permeability, we injected LY^{2-} into single, noncontacting astrocytes (*Materials and Methods*) and monitored its release over time. After detaching the pipette from the cell, we acquired images every 2 min; the rate of decay in fluorescence rapidly decreased to a more or less constant value indicating resealing (which required ~2 min). Cell labeling after dye injection was mainly diffuse, although as with uptake from the medium (Fig. S1), small puncta were evident in some cells (data not illustrated). On FGF-1 exposure, the rate of fluorescence decay was 5.5 ± 1.5 times control at 2 h and 6.8 ± 0.8 times control at 7 h (Fig. 1 *B* and *C*). After both 2-h and 7-h FGF-1 treatment, carbenoxolone (CBX) (0.2 mM), a Cx/Px HC blocker (8), reduced decay rates to the control level. (Unless otherwise stated, blockers were applied 15 min before the end of FGF-1 treatment and during the release or uptake measurements.) Octanol (Oct) (1 mM), which is closely related to heptanol, a Cx HC blocker that does not affect Px HCs (8), had no effect at 2 h and only partially blocked the decay after 7 h. Decay rates were variable and may have had a bimodal distribution after both 2- and 7-h FGF-1 treatment. Taken together, these data suggest that after 2 h of FGF-1 treatment, release of LY^{2-} is via Px HCs, probably activated by $P2X_7Rs$ (8, 26) and that after 7 h of FGF-1, release of LY^{2-} is via both Px HCs and Cx HCs.

To further elucidate the relative contribution of Px and Cx HCs to the membrane permeability induced by FGF-1, we measured Etd^+ uptake in confluent astrocytes. As noted above, Etd^+ uptake can be monitored in medium containing the dye, which allows simultaneous evaluation of uptake in 10–20 cells in a single experiment. After a 2-h FGF-1 treatment, the rate of Etd^+ uptake was about two times that in control (Fig. 1 *D* and *E*). Blockers of Cx HCs, heptanol, La^{3+} and Gd^{3+}, which have little effect on Px HCs (8), had no significant effect on Etd^+ uptake at this time; octanol also had no significant effect. In contrast, CBX (0.2 mM), which blocks both Cx and Px HCs, reduced uptake to the control level. Thus, Px HCs but not Cx HCs appear to mediate Etd^+ uptake after 2 h of exposure to FGF-1, and this result is in agreement with the results of decay of LY^{2-} fluorescence in single dye-injected cells. After a 7-h exposure to FGF-1, Etd^+ uptake was 3.8 ± 0.5 times faster than in control. The same Cx HC blockers reduced the increase in uptake by about half, and CBX reduced uptake to the control level (Fig. 1 *F* and *G*). Thus, at this time both Px and Cx HCs appear to contribute to dye uptake, although the degree of block with Cx HC blockers varied somewhat in the different experiments.

An inhibitor of FGFR1 tyrosine kinase, PD170374 (27), blocked both the Etd^+ uptake after 2 h and 7 h of FGF-1 treatment (application 45 min before FGF-1, Fig. S2) and the morphological changes induced by FGF-1 (as also shown by ref. 21, using the related compound, PD166866).

siRNA Knockdown of Px1 and Genetic Ablation of Cx43 Attenuate the Permeability Increase Induced by FGF-1. Cx43 is the main connexin expressed by spinal astrocytes in culture, and Px1 is also expressed by these cells (5) (Fig. S3). To establish the contribution of Px1 HCs and Cx43 HCs to the increase in membrane permeability, we used Cx43 KO mice (28), and a small interfering RNA against Px1 (siRNA Px1), which effectively blocks Px1 expression in mouse cortical astrocytes (26). Immunofluorescence and Western blot analysis established that this siRNA Px1 greatly reduced expression of Px1 in

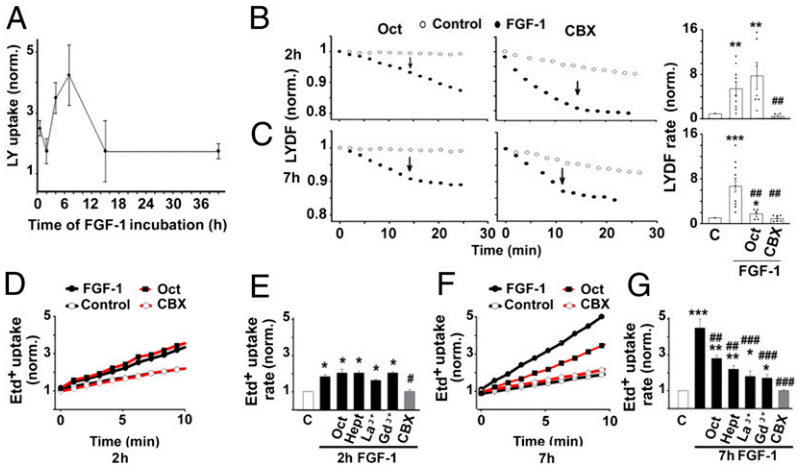

Fig. 1. FGF-1–induced permeabilization of spinal astrocytes is at first mediated by opening of Px HCs; then Cx HCs contribute. (*A*) LY^{2-} uptake evaluated as fluorescence intensity normalized to the control value in confluent cultures treated with FGF-1 for the indicated times. Representative images are in Fig. S1. (*B* and *C*) Decay in fluorescence following LY injection (LYDF) of isolated cells (images acquired every 2 min). LYDF under control conditions and after 2 h (*B*) or 7 h (*C*) FGF-1 treatment show the effect of 1 mM octanol (Oct), a Cx HC blocker, and 200 μM carbenoxolone (CBX), a Px and Cx HC blocker. Arrows indicate blocker application. Control and FGF-1–treated cells injected with LY^{2-} were in sister cultures used on the same day. LY^{2-} fluorescence was normalized to initial values. Bar graphs on the *Right* show quantitation; each point represents one cell. Decay rates and rates after drug application were normalized to rates at onset of measurement. [$^*P < 0.05$, $^{**}P < 0.01$, $^{***}P < 0.001$ vs. control; $^{\#\#}P < 0.01$ vs. FGF-1 treatment, 15 cells injected per condition (control and 2 h or 7 h of FGF-1), blockers, 6 cells injected per condition (FGF-1 + drug)]. (*D* and *F*) Uptake of Etd^+ in controls and after 2-h and 7-h FGF-1 treatment without or with Oct or CBX for the last 15 min of FGF-1 treatment and during uptake. (*E* and *G*) Uptake normalized to control for cells after 2 h or 7 h of FGF-1 without or with blockers applied for 15 min at the end of FGF-1 treatment and during uptake. HC blockers were octanol (Oct, 1 mM), heptanol (Hept, 1 mM), La^{+3} (200 μM), Gd^{+3} (200 μM), and carbenoxolone (CBX, 200 μM). ($^*P < 0.05$, $^{**}P < 0.01$, $^{***}P < 0.001$ vs. control; $^{\#}P < 0.05$, $^{\#\#}P < 0.01$, $^{\#\#\#}P < 0.005$ vs. FGF-1 alone; six experiments, 10 cells/experiment). Cx HC blockers had no effect after 2 h of FGF-1 and partially blocked uptake after 7 h of FGF-1. CBX blocked completely after both 2 h and 7 h of FGF-1.

rat spinal astrocytes (Fig. S3). A proprietary *Silencer* Select Negative Control oligonucleotide (Ambion) was used as a negative control.

Twenty-four hours after transfection with siRNA Px1, basal Etd^+ uptake was reduced (to 0.6 ± 0.2 times uptake by the control, $n = 4$, $P < 0.05$; untreated and negative-control treated were not significantly different, Fig. 2*A*). The basal uptake was not reduced significantly by applying octanol or CBX, suggesting that it was not mediated by HCs; possibly other mechanisms independent of Px HC opening but coupled to Px1 expression were involved (see ref. 8). After a 2-h FGF-1 treatment, Etd^+ uptake by siRNA Px1 transfected cells (normalized to that by control cells transfected with siRNA and without FGF-1 treatment) was less than uptake after a 2-h FGF-1 treatment by cells transfected with negative control (normalized to that by control cells transfected with negative control without FGF-1 treatment; ratio of siRNA to negative control: 0.54 ± 0.10, $n = 4$, $P < 0.05$) and somewhat greater than the uptake by the negative control with no FGF-1 treatment (Fig. 2*A*; 1.25 ± 0.05 times negative control, $n = 4$, $P < 0.05$). The small residual excess uptake is ascribable to incomplete block of Px1 expression (Fig. S3). After 7 h of FGF-1 treatment, uptake by siRNA Px1 transfected cells (normalized to that by control cells transfected with siRNA and without FGF-1 treatment) was less than uptake after a 7-h FGF-1 treatment by cells transfected with negative control (normalized to that by control cells transfected with negative control without FGF-1 treatment; ratio of siRNA to negative control: 0.69 ± 0.3, $n = 4$, $P < 0.05$) but greater than uptake by siRNA Px1 transfected cells after 2 h of FGF-1 treatment (2.33 ± 0.18, $n = 4$, $P < 0.05$); this increased uptake is ascribable to Cx43 HCs.

In astrocytes from Cx43 KO mice, basal uptake was comparable to that in cells from WT (1.07 ± 0.07 times WT, $n = 4$, $P > 0.05$, Fig. 2*B*). Uptake after 2 h of FGF-1 treatment was only slightly less in KO cells than in WT cells (1.61 ± 0.05 in KO and 1.85 ± 0.02 in WT times control, $n = 4$, $P < 0.05$ for both), in agreement with the inference of little contribution to uptake by Cx43 HCs at this time; the small difference observed is ascribable to altered expression of other genes in the Cx43 KO and reduction in intracellular ATP leading to reduced ATP release (29). After 7 h of FGF-1 treatment, uptake in KO cells (1.4 ± 0.15 times KO control, $P < 0.05$) was much less than that in WT (2.8 ± 0.7 times control, $P < 0.05$ WT vs. KO) and about the same as that after 2 h of FGF-1 treatment, consistent with lack of Cx43 HCs and continued Px1 mediation. These molecular data confirm that the membrane permeability depends primarily on Px1 HCs after 2 h of FGF-1 treatment and on both Px1 and Cx43 HCs after 7 h of FGF-1 treatment.

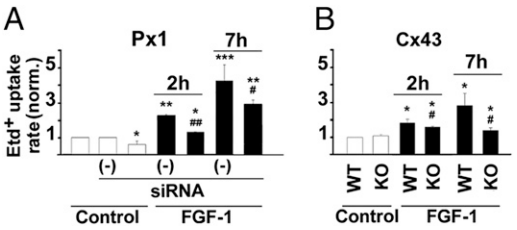

Fig. 2. FGF-1–induced permeabilization of spinal astrocytes depends on the expression of both Px1 and Cx43. (*A*) Rat astrocytes were transfected with siRNA against Px1 or with a negative control sequence. Transfected cells were untreated (controls in addition to untransfected cells) or treated for 2 h or 7 h with FGF-1. Uptake was normalized to the negative control (–) or to the siRNA control without FGF-1 treatment. siRNA Px1 reduced basal uptake (to 0.6 ± 0.2 times control, $P < 0.05$, $n = 3$). After 2-h FGF-1 treatment, normalized Etd^+ uptake in siRNA transfected cells was well below that in the negative control after 2-h FGF-1 treatment ($P < 0.01$) and slightly but significantly above that in the negative control without FGF-1 treatment ($P < 0.05$). After 7 h of FGF-1 treatment, normalized uptake in siRNA transfected cells was significantly less than that in the negative control after 7-h FGF-1 treatment ($P < 0.05$) but greater than that in the negative control without FGF-1 treatment ($P < 0.01$). (*B*) Astrocytes from wild-type and Cx43 KO mice were treated for 2 h or 7 h with FGF-1. Basal uptake did not differ significantly in the two groups. After 2 h of FGF-1 treatment Etd^+ uptake by Cx43 KO cells (normalized to that by untreated Cx43 KO astrocytes) was slightly less than in treated WT cells and greater than in control cells ($P < 0.05$). After 7 h of FGF-1 treatment, the uptake in Cx43 KO cells was about the same as after 2 h of FGF-1 (greater than in control, $P < 0.05$, and less than in WT, $P < 0.05$). In the siRNA experiments, Etd^+ uptake rate was evaluated in 10 cells per treatment group per experiment ($n = 3$ experiments). In the Cx43 KO experiments, Etd^+ uptake was measured in 7–10 cells per group ($n = 4$ experiments). In each case the uptake rates were normalized to the negative control or the siRNA control (rat) or WT or KO control (mice). $^*P < 0.05$, $^{**}P < 0.01$, $^{***}P < 0.001$ vs. control; $^{\#}P < 0.05$, $^{\#\#}P < 0.01$ FGF-1 WT vs. FGF-1 siRNA Px1 or Cx43 KO.

FGF-1 Activation of Px1 HCs Depends on Secreted ATP. We tested whether FGF-1–induced Etd^+ uptake by astrocytes was blocked by apyrase (APY), a soluble ATPase that would prevent autocrine and paracrine action of secreted ATP or by oxidized ATP (oATP), a general blocker of P2XRs. APY (2 mU/μL) or oATP (0.2 mM) applied for the last 15 min of a 2-h FGF-1 treatment and during uptake measurement completely prevented the increase in Etd^+ uptake (Fig. 3*A*). (The block by apyrase, which hydrolyzes ATP to ADP and then AMP, indicates that these hydrolysis products are not the active moiety). Thus, the action of FGF-1 in opening Px HCs is ATP- and P2XR-dependent and reversible during 15 min of apyrase or oATP application. Application of APY or oATP for the last 15 min of a 7-h FGF-1 treatment and during Etd^+ uptake only partially reversed the increase in uptake (Fig. 3*B*). Thus, the Px HC component of uptake is reversible in ~15 min or less, but the Cx HC component of uptake, which may involve insertion of HCs into the cell surface, either is not re-

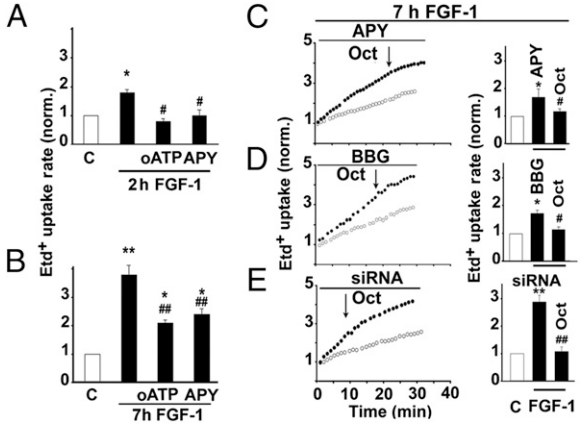

Fig. 3. Permeabilization induced after 2 h of FGF-1 treatment is mediated by autocrine/paracrine action of ATP acting on $P2X_7Rs$ to open Px1 HCs; after 7 h of FGF-1 treatment, a component is mediated by Cx HCs. (*A* and *B*) Etd^+ uptake rate in astrocytes after 2 h (*A*) or 7 h (*B*) of FGF-1 treatment, normalized to untreated control (*C*). The P2X blocker, oxidized ATP (oATP, 0.2 mM) or the ATPase, apyrase (APY, 2 mU/mL), were applied for the last 15 min of the FGF-1 treatment and during uptake measurement. After 2 h of FGF-1 treatment, uptake was reduced to control level by oATP and by APY. After 7 h of FGF-1 treatment, block by oATP and APY was only partial. (*C* and *D*) Experiments like those in *B* with Etd^+ uptake measured in cells under control conditions and after 7 h of FGF-1. APY or brilliant blue G (BBG, 10 μM) applied 15 min before and during uptake measurement partially reduced uptake; the residual uptake was reduced to near control by Oct applied at the arrows in the time course graphs. Quantitation is on the *Right*. (*E*) siRNA transfected cultures were treated with FGF-1 for 7 h, and Etd^+ uptake was measured in them and in control cultures. Oct (applied at arrow) reduced uptake to near the control level. Quantitation is on the *Right*. Each bar graph on the *Right* shows the Etd^+ uptake rate of three independent experiments (10 cells/experiment) under each condition. $^*P < 0.05$, $^{**}P < 0.01$ vs. control; $^{\#}P < 0.05$, $^{\#\#}P < 0.01$ FGF-1 alone vs. in the presence of APY or BBG or in siRNA transfected astrocytes.

NEUROSCIENCE

versible in 15 min or, as suggested below, is not entirely dependent on ATP and P2XR for its activation.

To characterize further this residual Etd^+ uptake after 7 h of FGF-1 with late block of ATP action, we applied 1 mM octanol after measurement of uptake for 10–20 min (Fig. 3 *C* and *D*, arrows). The component resistant to APY or brilliant blue G (BBG) was reduced to near control by 1 mM octanol. Similarly, uptake by astrocytes treated with siRNA Px1 and then 7 h of FGF-1 treatment was reduced to near control by octanol (Fig. 3*E*, arrow).

In support of FGF-1–induced ATP secretion, ATP levels in the culture medium were increased compared with control (Fig. S4*A*). This accumulation was due at least in part to ATP release through HCs, because APY and $P2X_7R$ and HC blockers reduced the effects of FGF-1.

To investigate the initial release of ATP in response to FGF-1, we applied botulinum neurotoxin A (BoNT A), which cleaves SNAP-25, a SNARE protein involved in vesicular release at many sites (30). BoNT A (200 ng/mL) applied 30 min before 7-h FGF-1 treatment largely prevented Etd^+ uptake. BoNT A significantly reduced uptake when applied at the start of FGF-1 treatment, but had little effect when applied at 1 h or 6 h during the 7-h FGF-1 treatment, although P2X blockers had marked effects when applied 15 min before the end of the 7-h treatment (Fig. 4). These data suggest that FGF-1 induces vesicular release of ATP and that this ATP triggers further and regenerative ATP release by inducing the opening of Px HCs; after Px HCs are open, vesicular release is not necessary to maintain ATP concentration. The effect of BoNT A was not uniform across cells. In 27 of 40 cells (four experiments) treated with BoNT A 0.5 h before the start of a 7-h FGF-1 treatment, the uptake was similar to that in controls, i.e., the effect of FGF-1 was completely blocked. In 13 of 40 cells, the uptake was comparable (approximately two times the control) to the component insensitive to apyrase after a 7-h FGF-1 treatment (Fig. 3*B* and below). This result is consistent with an FGF-1–induced increase in open Cx43 HCs independent of ATP in a fraction of the cells. Variability among cells was also indicated in the experiments on efflux of LY from dye injected cells (Fig. 1 *B* and *C*). Although the astrocytes have properties in common, molecular heterogeneity in culture may arise through stochastic differences in gene expression and signaling pathways (31, 32).

Exogenous ATP Increases Etd^+ Uptake. ATP, like FGF-1, increased Etd^+ uptake; 0.5 mM applied at 0, 2, and 4 h caused an increase in Etd^+ uptake evaluated 2 or 7 h after the first ATP application (Fig. S4 *C* and *D*). After initial release of ATP from vesicles in response to FGF-1, ATP-induced activation of Px1 HCs by $P2X_7Rs$ and then opening of Cx43 HCs would tend to maintain or increase ATP concentration. After a 2-h or 7-h application of 0.5 mM ATP (multiple applications as above) or 10 μM benzoyl ATP (BzATP, single application), a selective P2X agonist that is not hydrolyzed by ATPases, Etd^+ uptake (Fig. S4 *C–F*) was comparable to that by astrocytes treated with FGF-1 for the same time period (Fig. 1 *D–G*). Pharmacological evidence with the blockers used above indicated that the uptake was mediated by Px1 HCs at 2 h and by both Px1 and Cx43 HCs at 7 h. The Etd^+ uptake induced by ATP after 2 or 7 h was not affected by reactive blue 2 (RB2), a nonselective P2Y antagonist applied 15 min before uptake measurement, suggesting that P2Y receptors do not induce uptake (Fig. S4 *C* and *D*). (RB2 may also block $P2X_1$, $P2X_2$, $P2X_3$, but not $P2X_7$ receptors; refs. 33, 34).

The ATP-induced increase in uptake was completely inhibited in astrocytes treated with ATP + oATP for 7 h (following a 5-min pretreatment with oATP; data not shown), indicating that activation of P2X receptors is required for ATP-induced permeabilization. However, FGF-1 for 7 h applied with apyrase or oATP (preceded by a 5-min pretreatment with the same agent, Fig. S4*B*) did not completely block the increase in Etd^+ uptake. We presume the residual increase was Cx HC mediated and octanol sensitive, and, in agreement, the uptake after 7 h of FGF-1 treatment in siRNA Px1-treated cells was blocked by octanol (Fig. 3*E*). These data suggest that FGF-1 can activate some Cx HCs independently of ATP release and $P2X_7R$ activation.

The actions of P2XR or Px1 HC blockers and Cx HC blockers after 7 h of FGF-1 treatment demonstrated occlusion of the blocking actions in that antagonists of either type of HC could each block more than half the increase in permeability. In Fig. 1*B*, block by either BBG or Oct each reduced the LY^{2-} decay rate by more than half. In Fig. S4 *D* and *E*, block of Etd^+ uptake by either BBG or Oct was greater than half the block by CBX, which blocks both Px and Cx HCs. Rather than lack of specificity for the parallel uptake pathways, block of ATP release through Cx43 HCs may have reduced ATP activation of Px1 HCs. These results further support the inference that after 7 h of FGF-1 treatment, both Cx and Px HCs contributed to the increase in permeability.

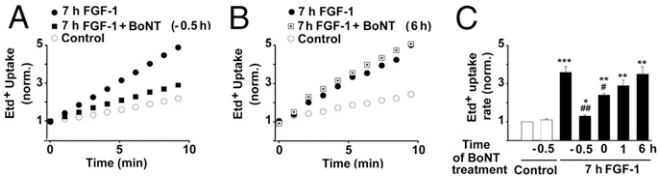

Fig. 4. FGF-1 initially causes ATP release by a vesicular mechanism as indicated by sensitivity to botulinum neurotoxin A (BoNT A). Subsequent release, as indicated by increase in Etd^+ uptake, is not terminated by BoNT A and presumably is self-maintaining through activation of $P2X_7Rs$ and Px1 HCs. (*A*) Spinal astrocytes pretreated with 200 ng/mL of BoNT A for 0.5 h before the start of a 7-h FGF-1 treatment showed uptake at 7 h near control and much less than that by cells treated with FGF-1 alone. (*B*) Application of BoNT A at 6 h after FGF-1 had no effect on Etd^+ uptake at 7 h. (*C*) Quantification of the time course of the BoNT A effect. BoNT A alone for 7.5 h had no effect on basal uptake. FGF-1–induced uptake was greatly reduced by BoNT A applied 0.5 h before the start of a 7-h FGF-1 treatment, was somewhat reduced by BoNT A applied at the start of treatment, and was not significantly affected by BoNT A applied at 1 or 6 h after the start of treatment. $^*P < 0.05$, $^{**}P < 0.01$, $^{***}P < 0.001$ FGF-1 vs. control; $^{\#}P < 0.05$, $^{\#\#}P < 0.01$ FGF-1 vs. FGF-1 + BoNT A.

FGF-1 Treatment Reduces Intercellular Coupling with Little Effect on Surface Cx43. FGF-1 modulation of coupling of spinal astrocytes was tested by iontophoretic injection of Etd^+ and by scrape loading with LY^{2-}. Astrocytes were microinjected with EtdBr (1 mM in 150 mM KCl) (Fig. S5). Control cells showed an incidence of dye coupling (percentage of cells coupled to one or more cells) of 72 ± 8.7% under control conditions ($n = 4$ experiments, 40 injections total). After 2- and 7-h FGF-1 treatments, the incidence of dye coupling between spinal astrocytes decreased to 38.0 ± 9.0% and 17.5 ± 9.5%, respectively ($P < 0.05$ vs. control for each duration, 2 h vs. 7 h, not significant).

In scrape loading, LY^{2-} spread from the edge of a cut was decreased to 27 ± 7% of control after a 7-h FGF-1 treatment, a decrease comparable to the effect of CBX (0.1 mM applied 15 min before loading) (to 22 ± 2% of control, $n = 4$, $P < 0.001$ vs. control for both FGF-1 and CBX, Fig. S6). Apyrase applied before and during a 7-h FGF-1 treatment (FGF-1 + APY) increased the extent of LY^{2-} spread to 70 ± 7% of control ($n = 4$, $P < 0.05$ vs. control, $P < 0.01$ vs. FGF-1 alone).

Astrocytes under control conditions or after a 7-h FGF-1 treatment displayed diffuse cytoplasmic Cx43 immunoreactivity and punctate labeling at cell interfaces (Fig. S7*A*). Labeling was not obviously affected by FGF-1, but some concentration around the nucleus may have been associated with activation and retraction of cytoplasm.

Western blot analysis of biotinylated surface and total proteins showed that FGF-1 treatment (7 h) reduced the level of total Cx43 to 60 ± 10% of control (Fig. S7*B*, $P < 0.05$, $n = 4$) and reduced the level of surface Cx43 (biotinylation, Biot) to 80 ± 8% of control (Fig. S7*B*, not significant, $P = 0.06$, $n = 4$). FGF-2 has similar effects on striatal and cortical astrocytes (35).

Discussion

Here, we demonstrate that spinal astrocytes in culture become permeable to LY^{2-} and Etd^{+} when treated with FGF-1. We attribute this permeabilization primarily to: (*i*) activation of FGFRs, (*ii*) which causes vesicular release of ATP; (*iii*) ATP-mediated activation of $P2X_7$Rs, which leads to (*iv*) opening of Px1 HCs and further release of ATP; and (*v*) by ~7 h, but not at 2 h, opening of Cx43 HCs as well, which also release ATP. Moreover, (*vi*) FGF-1 treatment causes a marked reduction in intercellular communication mediated by connexin GJs (Fig. 5). Our results may be specific to spinal astrocytes. Although FGF-2 decreases coupling in cortical as well as striatal astrocytes (35), FGF-1 did not permeabilize cortical astrocytes to Etd^{+}, although it caused the morphological changes associated with activation (Figs. S8 and S9).

To summarize the evidence, uptake by Px1 HCs at 2 h and both Px1 and Cx43 HCs at 7 h is indicated by the actions of HC blockers (Fig. 1); CBX blocked both classes of HC, whereas octanol and La^{3+} blocked only Cx HCs. The inferences were confirmed by the effects of siRNA Px1 and use of cells from Cx43 KO mice (Fig. 2). Mediation by ATP acting on P2XRs was indicated by block by apyrase and P2XR antagonists. Also, ATP or BzATP alone produced similar changes in permeability with comparable pharmacology (Fig. S4). FGF-1 initiated the permeability changes, and the permeability changes were prevented by PD170374, an FGFR-1 blocker (Fig. S2). FGF-1 caused vesicular release of ATP, indicated by block of permeabilization by BoNT A applied before FGF-1. However, BoNT A applied 1 h after FGF-1 had much less effect (Fig. 4), and evidently, ATP release became self-maintaining once Px1 HCs had opened; ATP released from Px1 HCs caused activation of $P2X_7$ receptors, opening of Px1 HCs, and further release of ATP that further activated $P2X_7$ receptors. Rise in Ca^{2+} caused by FGF-1 (36) or influx through P2XRs may have contributed to Px1 HC opening (11). Also, there may have been some opening of CxHCs by FGF-1 in a parallel, ATP-independent pathway (Fig. S4). FGF-1 caused a smaller reduction in dye coupling in the presence of apyrase, indicating a contribution by extracellular ATP (Fig. S6).

The action of ATP to open Px1 HCs is rapid in onset and rapidly reversible (<1 min) as indicated by electrophysiological measurement (8). In our experiments, apyrase or $P2X_7$R blockers applied 15 min before uptake abolished Px1 HC permeability, also indicating reversal of Px1 HC opening but at a poorer time resolution. However, the component blocked by Cx HC blockers was not greatly changed by this pretreatment. Thus, Cx HC opening is not as rapidly reversible.

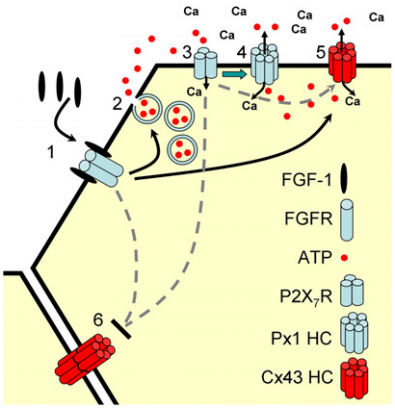

Fig. 5. Proposed reactions initiated by FGF-1. (*i*) FGF-1 binds to its (dimeric) receptor, likely causing a rise in cytoplasmic Ca^{2+}. (*ii*) ATP is released from vesicles, an action blocked by BoTN A. (*iii*) The ATP released acts on $P2X_7$Rs, which allows Ca^{2+} to enter. (*iv*) Activation of $P2X_7$Rs leads to opening of Px1 HCs (green arrow), allowing ATP release and Ca^{2+} entry. (*v*) Cx43 HCs are opened hours later, either through an action of FGF-1 or of $P2X_7$Rs and Px1 HCs. (*vi*) Gap junctional communication is reduced, an effect largely prevented by apyrase.

What mechanisms might explain the late involvement of Cx HCs in FGF-1 induced permeabilization? The response of $P2X_7$Rs to ATP desensitizes (37). However, the transient increase in $[Ca^{2+}]_i$ due to influx through $P2X_7$ receptors or release from intracellular stores activated via FGF-1 receptors can activate intracellular signaling proteins, such as kinases (36). In HeLa Cx43 transfectants, this early $[Ca^{2+}]_i$ signaling appears to be essential for the increase in membrane permeability and surface expression of Cx43 HCs observed after 7 h of FGF-1 treatment, because increase in both is abolished by intracellular Ca^{2+} chelation with BAPTA (38). However, in spinal astrocytes, increased permeability was accompanied by a minor reduction in surface Cx43 (Fig. S7), suggesting increase in Cx43 HC open probability. In cortical astrocytes, cytokines such as TNF-α and IL-1β induce cellular permeabilization but decrease the amount of surface Cx43 HCs; thus, the HC open probability must be increased; this process is mediated through a p38 MAPK-dependent mechanism (16). Activation of P2X or P2Y receptors can increase $[Ca^{2+}]_i$ leading to activation of p38 MAPK-dependent pathways (39, 40). In spinal astrocytes, action of blockers of P2YRs (i.e., RB2) and P2XRs (e.g., BBG) indicate that P2XRs mediated of permeabilization (Fig. 3 and Fig. S4).

FGF-1 treatment reduced dye coupling of spinal astrocytes. Cytokines and growth factors decrease connexin-mediated intercellular communication in astrocytes from some but not all brain areas (35). FGF-1 had much less effect on dye coupling in the presence of apyrase, implicating ATP as a major autocrine/paracrine mediator of the effect. In HeLa cells, decrease in coupling occurs without significant change in total Cx43 levels (38), and changes in phosphorylation state of Cx43 could decrease open probability of GJ channels as previously demonstrated for other growth factors (41). Decrease in the amount of Cx43 in GJs would not increase availability of Cx43 HCs, because junctional degradation involves proteolysis of entire cell–cell channels and not separation of HCs making them available for reuse (42).

GJs between astrocytes allow cooperation between the cells in maintaining the composition of the extracellular milieu of active neurons (43). Moreover, Px1 and Cx HCs play a number of important roles under physiological conditions, although opening of Cx HCs may accelerate cell death following insults such as metabolic inhibition (3), and Px1 HCs have been implicated in cell damage as well (7). We saw no reduction in astrocyte viability resulting from activation of $P2X_7$Rs and opening of Px1 and Cx43 HCs by FGF-1 or ATP; LY^{2-} uptake returned to near control levels after 15–40 h of FGF-1 treatment (Fig. 1*A*). However, in vivo extracellular ATP released from astrocytes could induce release of more ATP from microglia, at least in part through HCs (4), and enhance the inflammatory response acting as a paracrine signal to a different type of cell. Activated microglia also release other proinflammatory molecules including TNF-α and IL-1β that could act on astrocytes in concert with FGF-1 (which may be released by dying neurons) (21). Astrocyte Px1 and Cx HCs could release bioactive molecules and reduce net uptake of extracellular K^{+} and glutamate, leading to excitotoxicity (44); also, decreased coupling would hinder spatial buffering by astrocytes. Together, these changes could increase vulnerability of neighboring neurons, even those not directly affected by the initial insult (45). Thus, inhibition of $P2X_7$Rs and Px1 and Cx HCs may be therapeutic in spinal cord inflammation, and, recently, the $P2X_7$R antagonist, brilliant blue G, was shown to be neuroprotective in a rodent model of traumatic spinal cord injury (46).

Materials and Methods

Details are provided in *SI Materials and Methods*.

Materials. Culture media and serum were from Gibco BRL. FGF-1 (Sigma-Aldrich) was prepared as a 10 μg/mL stock solution in 5,000 UI/mL heparin.

Cell Cultures. Astrocytes from spinal cords of 1-d-old rat pups were prepared and cultured as described with minor modifications (21). Cultures were used after 15–20 d.

Lucifer Yellow and Ethidium Permeability Assay. Dye uptake was measured under control conditions and after treatment with FGF-1 and other reagents for various times. Uptake of Etd^+ and LY^{2-} was measured by brief application after treatment, or Etd^+ uptake was measured in time lapse in the presence of Etd^+. In other experiments, cells not in contact with other cells were injected with LY^{2-} through a pipette, and decay of fluorescence was monitored.

ATP Measurement. ATP in the culture medium was determined using a luciferin-luciferase kit (Molecular Probes) and luminometer (LUMIstar; BMG Labtech).

Dye Coupling. Coupling between confluent astrocytes in culture was evaluated in two ways, by iontophoretic injection of EtdBr into single cells and by scrape loading of lucifer yellow (LY^{2-}, ion MW 457.2) as described (47).

Immunofluorescence. Primary antibodies, a rabbit polyclonal anti-Cx43 antibody (48) and a chicken anti-Px1 C-terminal antibody (Millipore) were applied to ethanol-fixed astrocytes.

Surface Biotinylation and Western Blotting. Surface proteins were characterized by biotinylation, pull down with NeutrAvidin beads, and Western blotting as described (49).

siRNA Px1 and Cx43 KO. Cells were treated with siRNA targeting mouse pannexin 1 mRNA (sequence no. 3 in ref. 26). Cx43 KO mice (28) were obtained from D. C. Spray and E. Scemes (Albert Einstein College of Medicine, Bronx, NY).

Statistics. Data are presented as means ± SEM with the usual statistical tests and criterion $P < 0.05$ for significance. N was taken as the number of cells evaluated rather than the number of cultures, because the separate experiments gave the same results.

ACKNOWLEDGMENTS. We thank Dr. R. Radi for supplying us with the system to measure ATP (Free Radicals Center, Facultad de Medicina, Montevideo, Uruguay) and Dr. N. Alvarez, Gladys Garcés, and Adrianna Latuszek for technical assistance. Anti-Px1 antibody and siRNAs against Px1 were kindly supplied by Dr. Gerhard Dahl (University of Miami School of Medicine, Miami, FL). Drs. D. C. Spray and E. Scemes (Albert Einstein College of Medicine, Bronx, NY) provided the Cx43 knockout mice. This work was partially funded by Comisión Sectorial de Investigación Científica (CSIC) de la Universidad de la República Oriental del Uruguay, Montevideo, Uruguay (to V.A.), by Fundación Manuel Pérez-Facultad de Medicina, Montevideo, Uruguay (to V.A.), by the International Brain Research Organization (IBRO) (to J.M.G.), and AMSUD-PASTEUR (to J.M.G.), by Fondo Nacional de Desarrollo Científico y Tecnológico 1070591 and CONICYT-Anillo ATC 71 (to J.C.S.), by Linus Pauling Institute–Oregon State University (to P.C. and L.B.), and by National Institutes of Health Grants NS37402 and NS45287 (to M.V.L.B.) and NS036706 and HL084464 (to F.F.B.).

1. Söhl G, Willecke K (2004) Gap junctions and the connexin protein family. *Cardiovasc Res* 62:228–232.
2. Bennett MVL, Zukin RS (2004) Electrical coupling and neuronal synchronization in the mammalian brain. *Neuron* 41:495–511.
3. Bennett MVL, Contreras JE, Bukauskas FF, Sáez JC (2003) Gating and regulation of connexin 43 (Cx43) hemichannels. *Trends Neurosci* 26:610–617.
4. Orellana JA, et al. (2009) Modulation of brain hemichannels and gap junction channels by pro-inflammatory agents and their possible role in neurodegeneration. *Antioxid Redox Signal* 11:369–399.
5. Huang Y, Grinspan JB, Abrams CK, Scherer SS (2007) Pannexin1 is expressed by neurons and glia but does not form functional gap junctions. *Glia* 55:46–56.
6. Bruzzone R, Hormuzdi SG, Barbe MT, Herb A, Monyer H (2003) Pannexins, a family of gap junction proteins expressed in brain. *Proc Natl Acad Sci USA* 100:13644–13649.
7. MacVicar BA, Thompson RJ (2010) Non-junction functions of pannexin-1 channels. *Trends Neurosci* 33:93–102.
8. Ma W, Hui H, Pelegrin P, Surprenant A (2009) Pharmacological characterization of pannexin-1 currents expressed in mammalian cells. *J Pharmacol Exp Ther* 328:409–418.
9. Lai CP, et al. (2007) Tumor-suppressive effects of pannexin 1 in C6 glioma cells. *Cancer Res* 67:1545–1554.
10. Suadicani SO, Brosnan CF, Scemes E (2006) $P2X_7$ receptors mediate ATP release and amplification of astrocytic intercellular Ca2+ signaling. *J Neurosci* 26:1378–1385.
11. North RA (2002) Molecular physiology of P2X receptors. *Physiol Rev* 82:1013–1067.
12. Locovei S, Bao L, Dahl G (2006) Pannexin 1 in erythrocytes: Function without a gap. *Proc Natl Acad Sci USA* 103:7655–7659.
13. Riedel T, Schmalzing G, Markwardt F (2007) Influence of extracellular monovalent cations on pore and gating properties of $P2X_7$ receptor-operated single-channel currents. *Biophys J* 93:846–858.
14. Yan Z, et al. (2010) Experimental characterization and mathematical modeling of P2X7 receptor channel gating. *J Neurosci* 30:14213–14224.
15. De Vuyst E, et al. (2007) Connexin hemichannels and gap junction channels are differentially influenced by lipopolysaccharide and basic fibroblast growth factor. *Mol Biol Cell* 18:34–46.
16. Retamal MA, et al. (2007) Cx43 hemichannels and gap junction channels in astrocytes are regulated oppositely by proinflammatory cytokines released from activated microglia. *J Neurosci* 27:13781–13792.
17. Wang X, et al. (2004) $P2X_7$ receptor inhibition improves recovery after spinal cord injury. *Nat Med* 10:821–827.
18. Lin JH, et al. (2008) A central role of connexin 43 in hypoxic preconditioning. *J Neurosci* 28:681–695.
19. Koshinaga M, Sanon HR, Whittemore SR (1993) Altered acidic and basic fibroblast growth factor expression following spinal cord injury. *Exp Neurol* 120:32–48.
20. Reuss B, von Bohlen und Halbach O (2003) Fibroblast growth factors and their receptors in the central nervous system. *Cell Tissue Res* 313:139–157.
21. Cassina P, et al. (2005) Astrocyte activation by fibroblast growth factor-1 and motor neuron apoptosis: Implications for amyotrophic lateral sclerosis. *J Neurochem* 93:38–46.
22. Marchetto MC, et al. (2008) Non-cell-autonomous effect of human SOD1 G37R astrocytes on motor neurons derived from human embryonic stem cells. *Cell Stem Cell* 3:649–657.
23. Tardieu M, Gamby C, Avramoglou T, Jozefonvicz J, Barritault D (1992) Derivatized dextrans mimic heparin as stabilizers, potentiators, and protectors of acidic or basic FGF. *J Cell Physiol* 150:194–203.
24. Garré JM (2005) Connexins Hemichannels: Regulation by FGF-1 and ATP. Master's thesis [Programa para el Desarrollo de la Ciencias Basicas (PEDECIBA), Universidad de la Republica Oriental del Uruguay, Montevideo].
25. Contreras JE, et al. (2002) Metabolic inhibition induces opening of unapposed connexin 43 gap junction hemichannels and reduces gap junctional communication in cortical astrocytes in culture. *Proc Natl Acad Sci USA* 99:495–500.
26. Locovei S, Scemes E, Qiu F, Spray DC, Dahl G (2007) Pannexin1 is part of the pore forming unit of the $P2X_{(7)}$ receptor death complex. *FEBS Lett* 581:483–488.
27. Bansal R, Magge S, Winkler S (2003) Specific inhibitor of FGF receptor signaling: FGF-2-mediated effects on proliferation, differentiation, and MAPK activation are inhibited by PD173074 in oligodendrocyte-lineage cells. *J Neurosci Res* 74:486–493.
28. Reaume AG, et al. (1995) Cardiac malformation in neonatal mice lacking connexin43. *Science* 267:1831–1834.
29. Iglesias R, Dahl G, Qiu F, Spray DC, Scemes E (2009) Pannexin 1: The molecular substrate of astrocyte "hemichannels". *J Neurosci* 29:7092–7097.
30. Dolly JO, Aoki KR (2006) The structure and mode of action of different botulinum toxins. *Eur J Neurol* 13(Suppl 4):1–9.
31. Tay S, et al. (2010) Single-cell NF-kappaB dynamics reveal digital activation and analogue information processing. *Nature* 466:267–271.
32. Zhang Y, Barres BA (2010) Astrocyte heterogeneity: An underappreciated topic in neurobiology. *Curr Opin Neurobiol* 20:588–594.
33. Simon J, Webb TE, King BF, Burnstock G, Barnard EA (1995) Characterisation of a recombinant P2Y purinoceptor. *Eur J Pharmacol* 291:281–289.
34. Tuluc F, Bültmann R, Glänzel M, Frahm AW, Starke K (1998) P2-receptor antagonists: IV. Blockade of P2-receptor subtypes and ecto-nucleotidases by compounds related to reactive blue 2. *Naunyn Schmiedebergs Arch Pharmacol* 357:111–120.
35. Reuss B, Dermietzel R, Unsicker K (1998) Fibroblast growth factor 2 (FGF-2) differentially regulates connexin (cx) 43 expression and function in astroglial cells from distinct brain regions. *Glia* 22:19–30.
36. Munaron L (2002) Calcium signalling and control of cell proliferation by tyrosine kinase receptors (review). *Int J Mol Med* 10:671–676.
37. Roberts JA, et al. (2006) Molecular properties of P2X receptors. *Pflugers Arch* 452: 486–500.
38. Schalper KA, et al. (2008) Connexin hemichannel composition determines the FGF-1-induced membrane permeability and free [Ca2+]i responses. *Mol Biol Cell* 19:3501–3513.
39. Katz S, Boland R, Santillán G (2006) Modulation of ERK 1/2 and p38 MAPK signaling pathways by ATP in osteoblasts: Involvement of mechanical stress-activated calcium influx, PKC and Src activation. *Int J Biochem Cell Biol* 38:2082–2091.
40. Pfeiffer ZA, et al. (2004) The nucleotide receptor $P2X_7$ mediates actin reorganization and membrane blebbing in RAW 264.7 macrophages via p38 MAP kinase and Rho. *J Leukoc Biol* 75:1173–1182.
41. Warn-Cramer BJ, Lau AF (2004) Regulation of gap junctions by tyrosine protein kinases. *Biochim Biophys Acta* 1662:81–95.
42. Gaietta G, et al. (2002) Multicolor and electron microscopic imaging of connexin trafficking. *Science* 296:503–507.
43. Giaume C, McCarthy KD (1996) Control of gap-junctional communication in astrocytic networks. *Trends Neurosci* 19:319–325.
44. Ye ZC, Wyeth MS, Baltan-Tekkok S, Ransom BR (2003) Functional hemichannels in astrocytes: A novel mechanism of glutamate release. *J Neurosci* 23:3588–3596.
45. Ilieva H, Polymenidou M, Cleveland DW (2009) Non-cell autonomous toxicity in neurodegenerative disorders: ALS and beyond. *J Cell Biol* 187:761–772.
46. Peng W, et al. (2009) Systemic administration of an antagonist of the ATP-sensitive receptor P2X7 improves recovery after spinal cord injury. *Proc Natl Acad Sci USA* 106:12489–12493.
47. Giaume C, Marin P, Cordier J, Glowinski J, Premont J (1991) Adrenergic regulation of intercellular communications between cultured striatal astrocytes from the mouse. *Proc Natl Acad Sci USA* 88:5577–5581.
48. Brañes MC, Contreras JE, Sáez JC (2002) Activation of human polymorphonuclear cells induces formation of functional gap junctions and expression of connexins. *Med Sci Monit* 8:BR313–BR323.
49. Retamal MA, Cortés CJ, Reuss L, Bennett MVL, Sáez JC (2006) S-nitrosylation and permeation through connexin 43 hemichannels in astrocytes: Induction by oxidant stress and reversal by reducing agents. *Proc Natl Acad Sci USA* 103:4475–4480.